



Response of a land-terminating sector of the western Greenland Ice Sheet to early Holocene climate change: Evidence from ^{10}Be dating in the Søndre Isortoq region

Alia J. Lesnek*, Jason P. Briner

Department of Geology, University at Buffalo, Buffalo, NY 14260, USA

ARTICLE INFO

Article history:

Received 28 April 2017

Received in revised form

20 November 2017

Accepted 21 November 2017

Keywords:

Holocene

Greenland Ice Sheet

^{10}Be exposure dating

Moraines

ABSTRACT

The prevalence of land-terminating Greenland Ice Sheet margins is expected to increase as tidewater glaciers retreat onto land, yet few studies have characterized the sensitivity of these slow-moving margins to climatic variability. The response of land-terminating ice sheet sectors to climate forcing can be assessed by examining records of paleo-ice margin positions preserved in ice sheet moraine systems. In western Greenland, the extensive Fjord Stade moraine system was deposited by minor readvances or stillstands of the Greenland Ice Sheet margin during early Holocene net recession. Here, we combine new moraine mapping and cosmogenic ^{10}Be exposure dating to constrain the timing of Fjord Stade moraine deposition in the Søndre Isortoq region. We find that the Fjord Stade moraines are composed of a western stage and an eastern stage, which we constrain to 9.7 ± 0.7 ka ($n = 7$; 1 SD) and 9.0 ± 0.3 ka ($n = 7$; 1 SD), respectively. Synchronous deposition of the Fjord Stade moraine complex across at least 350 km of western Greenland implies a widespread response of the western Greenland Ice Sheet to the 9.3 ka event. Furthermore, these new moraine ages may correlate with Laurentide Ice Sheet-sourced freshwater pulses into the North Atlantic Ocean. We also show that the response of the western Greenland Ice Sheet to early Holocene freshwater forcing was not restricted to fast-flowing, marine-terminating outlet glaciers; the land-terminating margin in the Søndre Isortoq region halted or reversed its pattern of retreat in response to climatic change.

© 2017 Elsevier Ltd. All rights reserved.

1. Introduction

Over the past two decades, the rate of mass loss from the Greenland Ice Sheet (GrIS) has increased (Rignot et al., 2008; Shepherd et al., 2012; Enderlin et al., 2014). Much of this mass loss, particularly for Greenland's marine-terminating outlet glaciers, has been attributed to dynamic processes (e.g., calving) acting at the margins (Howat et al., 2007; Csatho et al., 2014; Aschwanden et al., 2016). Yet many dynamic processes, and the resultant effects on ice margin behavior and sea level rise, are poorly understood (Viel and Nick, 2011; Nick et al., 2013), which has led to large uncertainties about the long-term behavior of the GrIS under a rapidly changing climate (Pfeffer et al., 2008; Price et al., 2011; Bindshadler et al., 2013). In contrast, records of ice sheet fluctuations on land-terminating margins, which are

influenced to a lesser degree by ice dynamics than marine-terminating outlet glaciers (e.g., Sole et al., 2008), can help to reduce these uncertainties and provide additional information about the sensitivity of the GrIS to climate variability. Moreover, the prevalence of these slow-moving margins is expected to increase in the coming years as tidewater glaciers retreat onto land (Nick et al., 2013; Morlighem et al., 2014). Assessing how land-terminating margins of the GrIS have responded to abrupt climate change in the past is therefore important for informing models that predict the ice sheet's future behavior.

Moraines are a key source of information about the former extents of glaciers and ice sheets, and direct age control on moraines can constrain the magnitude and timing of past ice margin changes. In western Greenland, four major north-south trending moraine systems have been identified between the coast and the modern ice margin (Ten Brink, 1975), the most widely traceable of which are the Fjord Stade moraines (Weidick, 1968). Fjord Stade moraines are a nearly continuous moraine belt that spans approximately 600 km of western Greenland (Fig. 1; Weidick,

* Corresponding author.

E-mail address: alialesn@buffalo.edu (A.J. Lesnek).

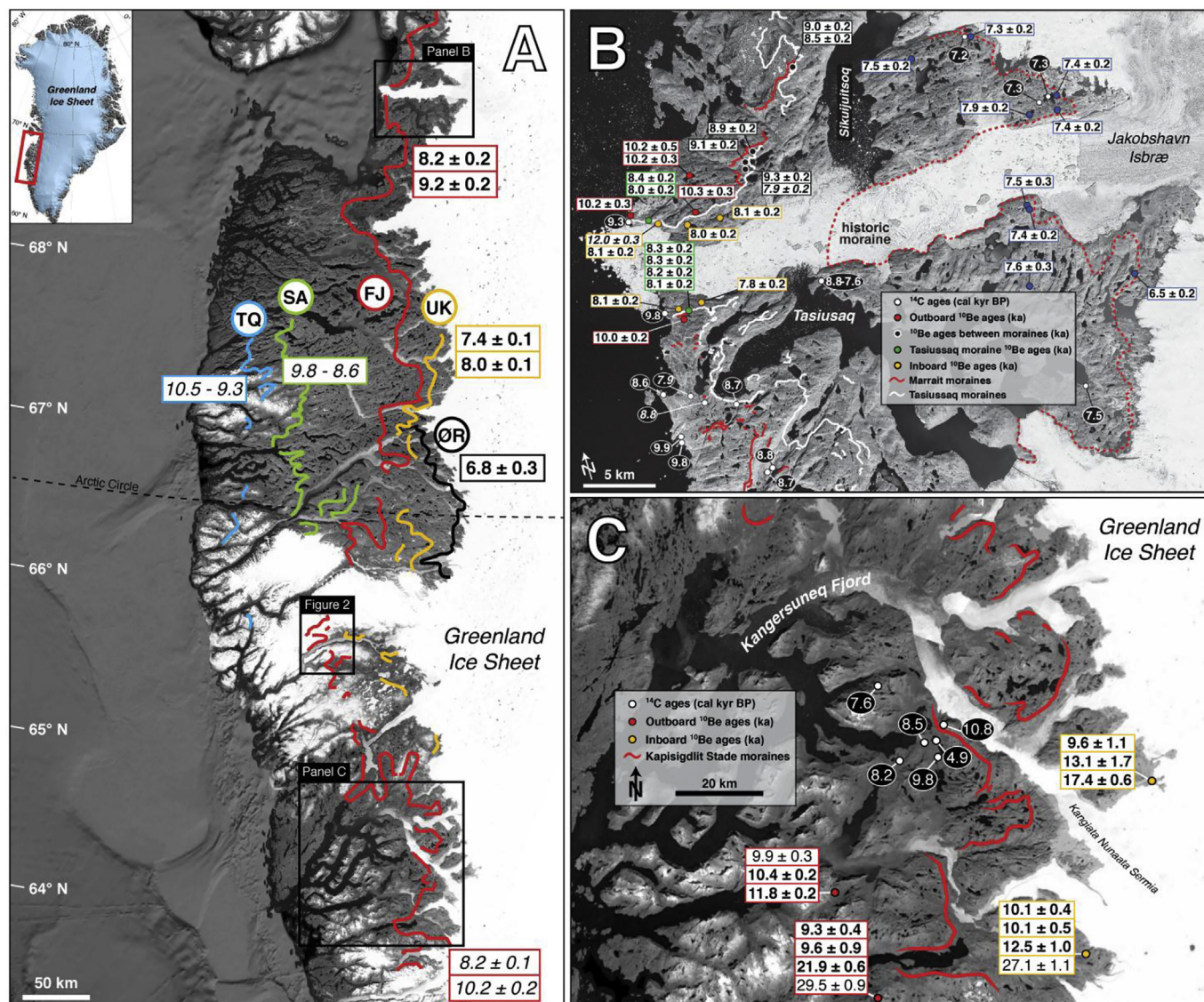


Fig. 1. (A) Major moraine systems in western Greenland (Weidick, 1968; Ten Brink, 1975). TQ = Taserqat; SA = Sarfartôq-Avatleq; FJ = Fjord Stade; UK = Umivît-Keglen; ØR = Ørkendalen. Age controls published prior to this study are shown in boxes. Bold text indicates direct age controls from ^{10}Be dating (Levy et al., 2012; Young et al., 2013a; Levy, 2014; Winsor et al., 2015a). Uncertainties are reported at 1SD. Italic text indicates indirect age controls on the moraines from ^{14}C dating and relative sea level curves (Weidick, 1972; Ten Brink, 1975; Larsen et al., 2014). (B) The Disko Bugt region and the Fjord Stade moraines (red and white lines; Weidick, 1968). Age controls on the moraines are from ^{14}C dating (cal kyr BP; white dots) and ^{10}Be dating (ka, 1 SD; Corbett et al., 2011; Young et al., 2013a). (C) The Kangersuneq Fjord region and the Kapisigdlit Stade moraines (red lines; Weidick et al., 2012). Existing age controls on the moraines are from ^{14}C ages (cal kyr BP; white dots; Weidick et al., 2012), and ^{10}Be ages (ka) from outside (red dots) and inside (yellow dots) the moraines (Larsen et al., 2014). Normal and bold fonts in the white boxes refer to boulder and bedrock ^{10}Be ages, respectively. (For interpretation of the references to colour in this figure legend, the reader is referred to the web version of this article.)

1968). Radiocarbon ages across western Greenland broadly constrain the timing of Fjord Stade moraine deposition to the early Holocene (e.g., Ten Brink, 1975), but direct age control on the moraines has only been obtained along primarily marine-terminating margins in the Disko Bugt region (Young et al., 2013a). Farther south, along a marine-terminating margin in the Kangersuneq Fjord region, two separate studies reached different conclusions about the age of these moraines (Weidick et al., 2012; Larsen et al., 2014). Consequently, questions concerning the processes driving Fjord Stade moraine formation across large areas of western Greenland remain unresolved. Do these moraines represent a large-scale response of the western GrIS to early Holocene abrupt climate change (Alley et al., 1997; Fleitmann et al., 2008; Young et al., 2013a), even along land-terminating margins that are far removed fast-flowing outlet glaciers? Or, alternatively,

are the moraines of little climatic significance (Warren and Hulton, 1990; Long et al., 2006)?

Here, we reconstruct the early Holocene history of a land-terminating ice sheet margin in the Søndre Isortoq region of western Greenland. This area contains an extension of the Fjord Stade moraine belt that stretches from Disko Bugt to Kangersuneq Fjord (Weidick, 1968; Funder et al., 2011), and is far from locations where the Fjord Stade moraines have been previously dated (e.g., Weidick et al., 2012; Young et al., 2013a). By obtaining new ^{10}Be exposure age constraints on the moraines in the Søndre Isortoq region, we test the hypothesis that the Fjord Stade moraines record a widespread response of the western GrIS to early Holocene abrupt cooling events. Furthermore, we assess the sensitivity of land-terminating GrIS margins to abrupt climate change.

2. Regional setting

Situated ~90 km east of the Greenland coast, the Søndre Isortoq region is amidst one of the most extensive tracts of ice-free terrain in Greenland (Fig. 1). Uplands in the Søndre Isortoq region host the Sukkertoppen and Qarajugtoq ice caps (Kelly and Lowell, 2009). Cosmogenic $^{26}\text{Al}/^{10}\text{Be}$ ratios from near the modern ice caps suggest that high-elevation areas in the Søndre Isortoq region were covered by cold-based, minimally erosive ice for much of the middle and late Quaternary (Beel et al., 2016). These ice caps were confluent with the GrIS during Last Glacial Maximum (26–19 ka; Clark et al., 2009) and early Holocene (Weidick, 1968) but are independent of the modern ice sheet. The upland areas of the Søndre Isortoq region are separated by low-lying valleys that contain ice-sculpted gneissic bedrock, erratic boulders perched on bedrock, lakes, and well-defined moraine ridges mapped as part of the Fjord Stade moraine belt (Weidick, 1968).

Ice retreat from the shelf in areas north and south of the Søndre Isortoq region occurred between ~15 and 10 cal kyr BP (Bennike and Björck, 2002; Kelley et al., 2015; Winsor et al., 2015b). Retreat from the present day coastline in the Sisimuit region may have begun as early as 14.4 ka¹ (Winsor et al., 2015a), followed by thinning from a hypothesized maximum elevation of ~750 m above sea level (asl; Roberts et al., 2009). Minimum-limiting ^{14}C and ^{10}Be ages near the present coastline west of our study area indicate that GrIS retreated out of Baffin Bay prior to ~11.0–10.5 ka (Roberts et al., 2009; Bennike et al., 2011).

Retreat of the western GrIS during the Holocene was punctuated by stillstands or minor readvances in the Sisimuit-Kangerlussuaq region that resulted in suite of north-south trending moraine systems between the present coastline and the modern GrIS margin (Fig. 1). Based on geomorphological mapping and radiocarbon dating, Ten Brink (1975) identified five major moraine systems, and from oldest to youngest, they are known as (1) the Taserqat moraines, (2) the Sarfartôq-Avatdlek moraines, (3) the Fjord Stade moraines, (4) the Umîvît-Keglen moraines, and (5) the Ørkendalen moraines. These “moraine systems”, which are often composed of many individual moraine crests, are differentiated from “local moraines” on the basis of several criteria, including their lateral extent and their similar ages across the region, suggesting that each moraine system represents a “regionally synchronous ice-margin position” (Ten Brink, 1975). Subsequent analyses of ice margin deposits from the coast to the Kangerlussuaq region show that the deposition of moraines in western Greenland was somewhat continuous throughout the early and middle Holocene (Van Tatenhove, 1995), although the fragmented nature of many of these moraines may disqualify them from classification as “moraine systems” according to the strict criteria proposed by Ten Brink (1975). More recently, high-resolution mapping has revealed a multitude of smaller, discontinuous moraine ridges independent of the major moraine near the modern ice margin in the Kangerlussuaq region (Carrivick et al., 2017), highlighting the complexity and spatial variability of the area's ice margin history.

Situated near the modern coastline, the Taserqat moraines are the oldest moraine system in the Sisimuit-Kangerlussuaq region. The age of these moraines has not been directly determined, but Weidick (1972) tentatively assigned them an age of 10.5–9.3 cal kyr BP based on their relationship to relative sea level.

The formation of the Sarfartôq-Avatdlek moraine system is constrained by radiocarbon ages to 9.8–8.6 cal kyr BP (Ten Brink, 1975). It is unclear if the GrIS margin experienced a stillstand or minor readvance to deposit these moraines. Following Sarfartôq-Avatdlek moraine deposition, the GrIS retreated at an average rate of $35 \pm 5 \text{ m a}^{-1}$. This retreat was oscillatory, producing discontinuous moraines that are restricted to local valleys (Ten Brink, 1975).

Based on radiocarbon dated shells, Weidick (1972) constrained the timing of Fjord moraine deposition to 9.1–7.9 cal kyr BP. This interval generally aligns with the age of the Fjord Stade moraines in the Disko Bugt region, where two widely traceable moraine crests (the Marrait and Tasiussaq moraines) have been dated to 9.2 and 8.2 ka with ^{10}Be exposure dating (Fig. 1B; Young et al., 2013a), suggesting a link to abrupt cooling events recorded in Greenland ice cores and elsewhere (e.g., Alley et al., 1997; Rasmussen et al., 2007; Fleitmann et al., 2008). The Fjord Stade moraines in the Søndre Isortoq region are also expressed as two sets of moraine crests, described as a “western stage” and an “eastern stage,” and were suggested to have formed in response to periods of lower atmospheric temperatures during the early Holocene (Weidick, 1968), but this hypothesis is untested. Retreat from the Fjord moraines was also oscillatory, resulting in numerous discontinuous moraines and some stagnant ice features such as kettles and kame terraces (Ten Brink, 1975).

Overall retreat from the Fjord moraines was punctuated by deposition of the Umîvît-Keglen moraine system. Chronological controls on the Umîvît-Keglen moraine system are inconsistent; ^{10}Be dating of the same moraine crests has yielded ages of $7.4 \pm 0.1 \text{ ka}$ ($n = 6$; Levy, 2014) and $8.0 \pm 0.1 \text{ ka}$ ($n = 3$; Winsor et al., 2015a). Winsor et al. (2015a) suggested the Umîvît-Keglen moraines may have formed in response to the 8.2 ka cooling event, similar to the younger Fjord Stade moraine in the Disko Bugt region (Young et al., 2013a). Retreat from the Umîvît-Keglen moraines was “slow but progressive” (Ten Brink, 1975).

The Ørkendalen moraines are the youngest of the five Holocene moraine systems in the Sisimuit-Kangerlussuaq region. Levy et al. (2012) constrained the age of these moraines, which lie just outside the modern ice margin, to $6.8 \pm 0.3 \text{ ka}$ ($n = 9$) with ^{10}Be dating. Be-10 ages just inside the Ørkendalen moraines show that the GrIS retreated within its present extent after $6.8 \pm 0.2 \text{ ka}$ ($n = 7$; Carlson et al., 2014).

The early Holocene history of the southwestern GrIS near Kangersuneq Fjord (Fig. 1C) is broadly similar to that of the Kangerlussuaq region. Evidence from ^{10}Be dating indicates that the coast became ice-free ~10.5 ka (Larsen et al., 2014). Overall recession of the GrIS continued during the early Holocene, but this retreat slowed or possibly reversed during the deposition of the Kapisigdlit Stade moraines, a major moraine system 10–30 km from the modern ice margin (Weidick, 1968; Ten Brink and Weidick, 1974; Kelly, 1985). These moraines have been hypothesized to be Fjord Stade equivalents (Weidick, 1968), but recent efforts to date the moraines have yielded conflicting results. Using a relative sea level curve for the Kangersuneq region and a 50 m asl marine terrace that potentially crosscuts the moraines, Weidick et al. (2012) assigned the Kapisigdlit Stade moraines an age of 8.1–8.3 cal kyr BP. A shell of the bivalve *Macoma calcarea* dated to 11.1–10.6 cal kyr BP was found embedded in the proximal side of a Kapisigdlit Stade moraine, suggesting the moraines were deposited during a readvance of the ice margin, perhaps during the 8.2 ka abrupt cooling event (Weidick et al., 2012). This result, along with ^{10}Be ages from the younger Fjord Stade moraine in Disko Bugt (Young et al., 2013a), implies a widespread response of the western GrIS to the 8.2 ka event. However, based on the marine limit on either side of the moraines and deglaciation ages derived from ^{10}Be dating of high elevation erratic boulders, Larsen et al. (2014) argue the Kapisigdlit

¹ All ^{10}Be ages reported here have been recalculated using version 3 of the CRONUS-Earth online exposure age calculator (http://hess.ess.washington.edu/math/index_dev.html), Lm scaling, and the Baffin Bay/Arctic ^{10}Be production rate (Young et al., 2013b). Uncertainties are reported at 1 SD for individual sample ages as well as average ages.

Stade moraines were instead deposited between 10.4 cal kyr BP and 10.1 ± 0.4 ka. It should be noted, however, that neither of these studies *directly* dated the Kapisigdlit Stade moraines. Consequently, the age of these moraines, and their relationship to the Fjord Stade moraines in the Disko Bugt and Søndre Isortoq regions, remains an open question.

3. Material and methods

To constrain the age of the eastern and western stages of the Fjord Stade moraines in the Søndre Isortoq region, we dated 24 boulders from two sites: Lûtiviup Nunatarssua and Qátqatsiaq (Fig. 2). To provide bracketing ages on the moraines, we collected nine perched boulders beyond (west of) the moraines, and six perched boulders inside (east) of the moraines. Boulders were generally perched on or near striated bedrock surfaces. At Lûtiviup Nunatarssua, too few suitable boulders for ^{10}Be dating existed directly on the moraine crests, so our age constraints are maximum and minimum values derived from the perched boulders outside and inside of the moraines. At the Qátqatsiaq site, we dated seven moraine boulders. Samples were collected from the upper several centimeters of large, stable boulders using a rock saw, hammer, and chisel. We avoided the edges of boulders and collected material from flat upper surfaces. A clinometer was used to measure topographic shielding and a handheld GPS receiver with an approximate vertical uncertainty of ~5 m was used to record the sample coordinates and elevations. Sample elevations range from 495 to 785 m asl, well above the local marine limit of ~120 m asl (Sugden, 1972; Ten Brink and Weidick, 1974).

Moraine crests were mapped throughout the field area using aerial photographs acquired in 1985 by the Geological Survey of

Denmark and Greenland (scale 1:150,000). Additional moraine crest mapping in the Søndre Isortoq region was conducted using v2.0 (release 4) of ArcticDEM (<http://pgc.umn.edu/arcticdem>), a publicly available digital elevation model with a 2 m horizontal resolution. We traced moraine crests northwards from Qátqatsiaq valley to Lûtiviup Nunatarssua, just southeast of the Sukkertoppen Ice Cap (Fig. 2). These maps were validated in the field by walking along portions of the moraines with a handheld GPS that continuously recorded our position. Our moraine mapping generally agrees with previously published maps of the Fjord Stade moraines (Weidick, 1968, 1985; Ten Brink, 1975), although we differentiate here between major moraine complexes and local moraines using the criteria proposed by Ten Brink (1975).

Samples underwent physical and chemical preparation at the University at Buffalo Cosmogenic Isotope Laboratory using procedures modified from Kohl and Nishiizumi (1992). Samples were crushed and sieved to separate the 425–850 μm size fraction, magnetically separated, and etched in dilute HCl and HF/HNO₃ acid solutions. Quartz-rich material was isolated by lithium heteropolytungstate heavy liquid separation followed by additional HF/HNO₃ etches until the desired quartz purity was achieved. Quartz purity was measured by inductively coupled plasma optical emission spectroscopy at the University of Colorado, Boulder.

Beryllium was isolated from quartz following procedures adapted from the University of Vermont Cosmogenic Nuclide Laboratory (Corbett et al., 2016). Samples were processed in batches of 12 (including one process blank) and spiked with ~222–228 μg of ^9Be carrier solution prepared from phenakite mineral (GFZ German Research Center for Geosciences “Phenakite” standard, ^9Be concentration 372.5 ± 3.5 ppm; Table 1). We used anion and cation exchange columns to isolate Be, and BeOH was precipitated in a pH 8 solution. The BeOH gels were oxidized to BeO, mixed with Nb powder, and packed into stainless steel cathodes for accelerator mass spectrometry (AMS) analysis.

All $^{10}\text{Be}/^9\text{Be}$ ratios were measured at the Center for Accelerator Mass Spectrometry at Lawrence Livermore National Laboratory and normalized to standard 07KNSTD3110, which has an assumed $^{10}\text{Be}/^9\text{Be}$ ratio of 2.85×10^{-12} (Nishiizumi et al., 2007). Sample ratios were corrected using batch-specific blank values that ranged from 1.11×10^{-15} to 3.98×10^{-15} ($n = 5$). AMS analytical uncertainty ranged from 1.2 to 3.8%.

^{10}Be exposure ages (Table 1) were calculated with the online CRONUS-Earth exposure age calculator version 3 (http://hess.ess.washington.edu/math/index_dev.html; Balco et al., 2008) using the regionally calibrated Baffin Bay/Arctic ^{10}Be production rate (Young et al., 2013b) and the Lal/Stone time-varying scaling scheme (Lal, 1991; Stone, 2000). This production rate has been used extensively to calculate exposure ages in Greenland (e.g., Kelley et al., 2015; Beel et al., 2016; Larsen et al., 2016; Sinclair et al., 2016) and is similar to independently-derived ^{10}Be production rates from other regions (Balco et al., 2009; Putnam et al., 2010). Ages calculated using alternative production rates and scaling schemes are reported in Table 2. Because few constraints on Holocene relative sea level change exist for the broader Søndre Isortoq region, uncertainties about the elevation history of our samples and the relatively minor effect of estimated elevation adjustments (<1%) lead us to report our ^{10}Be exposure ages without elevation corrections. We made no corrections for snow shielding or erosion. Samples were collected from windswept topographic highs and we found no correlation between boulder height and ^{10}Be age, suggesting the boulders have not experienced significant snow cover. We observed glacial polish on bedrock in the field area, which implies minimal erosion of rock surfaces since deglaciation. We therefore assume erosion on sample surfaces to be negligible.

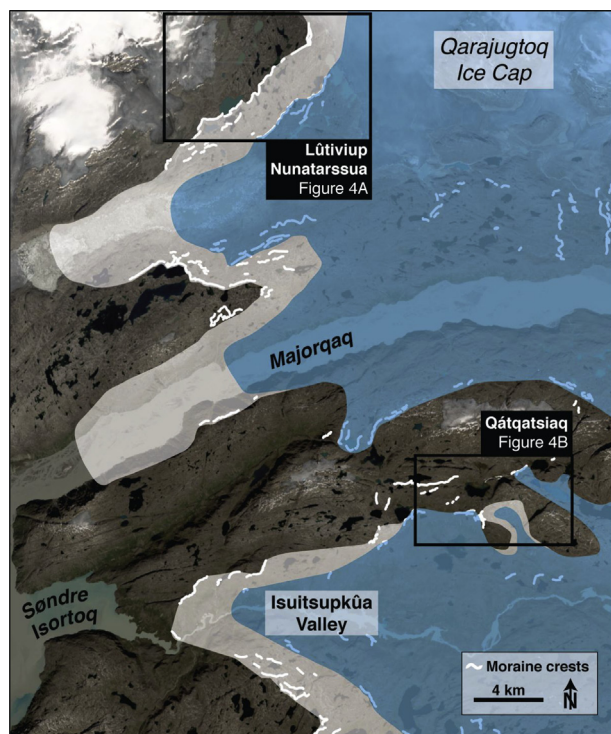


Fig. 2. Map of early Holocene moraines (white lines) in the Søndre Isortoq region with sites for ^{10}Be dating at Lûtiviup Nunatarssua and Qátqatsiaq (black boxes). Shading indicates GrIS configuration during formation of the western (white) and eastern (blue) stages of the Fjord Stade moraines. Base image: Landsat 8. (For interpretation of the references to colour in this figure legend, the reader is referred to the web version of this article.)

Table 1¹⁰Be sample information for the Søndre Isortoq region.

Sample	Sample type	Latitude (°N)	Longitude (°W)	Elevation (m asl)	Boulder height (m)	Sample thickness (cm)	Topographic shielding correction	Quartz (g)	⁹ Be added (μg)	¹⁰ Be/ ⁹ Be ratio ^a	¹⁰ Be (1E+04 * atoms/g)	¹⁰ Be age (ka) ^b
Outboard of moraines, both sites												
14GROR-04	Perched boulder	65.8354	51.7284	495	1.3	2.0	0.99872	26.12	225	1.27E-13 ± 2.69E-15	7.32 ± 0.16	10.4 ± 0.2
14GROR-05	Perched boulder	65.8352	51.7282	538	0.6	2.0	0.99809	22.33	226	1.67E-13 ± 5.33E-15	11.31 ± 0.36	15.4 ± 0.5
14GROR-09	Perched boulder	65.8634	51.6145	640	0.5	1.5	0.99931	25.09	228	1.39E-13 ± 2.54E-15	8.45 ± 0.15	10.4 ± 0.2
14GROR-19	Perched boulder	65.6747	51.2542	772	1.6	2.0	0.99801	18.04	226	1.13E-13 ± 2.20E-15	9.49 ± 0.19	10.4 ± 0.2
14GROR-20	Perched boulder	65.6747	51.2558	785	0.9	2.0	0.99897	20.99	227	1.25E-13 ± 3.18E-15	9.01 ± 0.23	9.9 ± 0.3
14GROR-21	Perched boulder	65.6744	51.2727	689	2.4	2.0	0.99420	18.98	227	1.08E-13 ± 3.07E-15	8.58 ± 0.48	10.2 ± 0.6
14GROR-22	Perched boulder	65.6780	51.2842	756	0.9	2.0	0.99873	18.20	226	1.08E-13 ± 3.07E-15	9.01 ± 0.26	10.1 ± 0.3
14GROR-25	Perched boulder	65.6584	51.3626	525	1.1	2.0	0.99907	29.99	226	1.50E-13 ± 2.96E-15	7.57 ± 0.15	10.4 ± 0.2
14GROR-38	Perched boulder	65.6618	51.3555	629	0.9	3.0	0.99643	18.36	227	9.35E-14 ± 2.69E-15	7.73 ± 0.22	9.8 ± 0.3
Between moraines, Lûtiviup Nunatarssua												
14GROR-10	Perched boulder	65.8555	51.6153	619	1.0	2.0	0.99998	25.27	228	1.21E-13 ± 2.41E-15	7.32 ± 0.15	9.2 ± 0.2
14GROR-11	Perched boulder	65.8472	51.6320	609	1.2	2.0	0.99985	30.76	226	1.49E-13 ± 3.21E-15	7.34 ± 0.16	9.4 ± 0.2
14GROR-12	Perched boulder	65.8245	51.6904	501	0.9	2.0	0.99751	30.61	227	1.31E-13 ± 3.12E-15	6.50 ± 0.16	9.2 ± 0.2
Western stage, Qâtqatsiaq												
14GROR-36	Moraine boulder	65.6512	51.3503	590	2.0	2.0	0.99017	30.10	227	1.46E-13 ± 2.75E-15	7.35 ± 0.14	9.6 ± 0.2
14GROR-37	Moraine boulder	65.6509	51.3502	592	1.0	2.0	0.99017	28.93	227	1.46E-13 ± 3.03E-15	7.66 ± 0.16	10.0 ± 0.2
Eastern stage, Qâtqatsiaq												
14GROR-29	Moraine boulder	65.6515	51.3573	564	2.2	2.5	0.99731	30.10	227	1.28E-13 ± 2.52E-15	6.45 ± 0.12	8.6 ± 0.2
14GROR-30	Moraine boulder	65.6512	51.3561	573	0.8	2.0	0.99731	30.01	226	1.41E-13 ± 2.71E-15	7.08 ± 0.14	9.4 ± 0.2
14GROR-31	Moraine boulder	65.6512	51.3503	590	2.0	3.0	0.98265	27.82	222	1.23E-13 ± 2.39E-15	6.55 ± 0.13	8.7 ± 0.2
14GROR-32	Moraine boulder	65.6511	51.3504	591	1.4	2.0	0.98333	30.32	227	1.35E-13 ± 2.62E-15	6.77 ± 0.13	8.9 ± 0.2
14GROR-33	Moraine boulder	65.6510	51.3504	593	0.8	2.0	0.98119	30.31	227	1.36E-13 ± 2.35E-15	6.82 ± 0.12	9.0 ± 0.2
14GROR-34	Moraine boulder	65.6509	51.3502	592	1.4	2.0	0.98333	30.14	227	1.41E-13 ± 3.44E-15	7.08 ± 0.17	9.3 ± 0.2
14GROR-35	Moraine boulder	65.6508	51.3501	593	0.6	2.0	0.98333	26.40	226	1.20E-13 ± 2.09E-15	6.88 ± 0.12	9.1 ± 0.2
Inboard boulders, Qâtqatsiaq												
14GROR-26	Perched boulder	65.6521	51.3740	506	0.5	2.0	0.99972	29.46	228	1.21E-13 ± 2.30E-15	6.28 ± 0.12	8.8 ± 0.2
14GROR-27	Perched boulder	65.6523	51.3736	529	1.9	2.0	0.99972	30.86	228	1.34E-13 ± 2.30E-15	6.60 ± 0.11	9.1 ± 0.2
14GROR-28	Perched boulder	65.6520	51.3722	533	2.0	1.5	0.99972	30.16	226	1.31E-13 ± 2.52E-15	6.58 ± 0.13	9.0 ± 0.2

^a AMS results are standardized to 07KNSTD3110 (Nishiizumi et al., 2007); ratios are blank-corrected and shown at 1-sigma uncertainty.^b Be ages reported at 1-sigma AMS uncertainties and calculated using the Arctic/Baffin Bay production rate (Young et al., 2013b) and Lm scaling.

4. Results

4.1. Moraine mapping

Following the moraine classification system proposed by Ten Brink (1975), the moraine systems at Lûtiviup Nunatarssua are composed of well-defined, single-crested ridges that protrude roughly 5 m above the surrounding landscape (Fig. 3). Two distinct sets of NE-SW-trending moraine crests are present at this site (Fig. 2; Weidick, 1968), and all moraines are draped over bedrock

with discontinuous till cover. We observed multiple outcrops of glacially-polished bedrock both beyond and inside the moraine.

At Qâtqatsiaq, we mapped moraine systems composed of several nested moraine crests. The crests are well-defined and clast-supported in places (Fig. 3). We observed minimal till cover at this site; the moraines are instead draped directly over ice-sculpted bedrock. In contrast to the moraines at Lûtiviup Nunatarssua, the moraines at Qâtqatsiaq are fragmented, likely due to erosion by outwash. The moraines at Qâtqatsiaq are interpreted as right lateral moraines associated with an ice lobe that filled Isuitsupkûa valley

Table 2¹⁰Be ages calculated with alternative production rates and scaling schemes.

Sample	¹⁰ Be ages: Arctic/Baffin Bay Production Rate ^a (ka)				¹⁰ Be ages: Default CRONUS Production Rate ^b (ka)					
	Constant (St)	Percent change ^c	LSDn	Percent change ^c	Constant (St)	Percent change ^c	Time-varying (Lm)	Percent change ^c	LSDn	Percent change ^c
Outboard of moraines, both sites										
14GROR-04	10.4 ± 0.2	0%	10.6 ± 0.2	2%	10.3 ± 0.2	1%	10.0 ± 0.2	4%	9.7 ± 0.2	7%
14GROR-05	15.5 ± 0.5	1%	15.8 ± 0.5	3%	15.2 ± 0.5	1%	14.8 ± 0.5	4%	14.4 ± 0.5	6%
14GROR-09	10.4 ± 0.2	0%	10.6 ± 0.2	2%	10.3 ± 0.2	1%	10.0 ± 0.2	4%	9.7 ± 0.2	7%
14GROR-19	10.5 ± 0.2	1%	10.6 ± 0.2	2%	10.3 ± 0.2	1%	10.2 ± 0.2	2%	9.7 ± 0.2	7%
14GROR-20	9.8 ± 0.3	1%	10.0 ± 0.3	1%	9.7 ± 0.2	2%	9.4 ± 0.2	5%	9.1 ± 0.2	8%
14GROR-21	10.2 ± 0.5	0%	10.4 ± 0.6	2%	10.0 ± 0.6	2%	9.8 ± 0.6	4%	9.5 ± 0.5	7%
14GROR-22	10.0 ± 0.3	1%	10.2 ± 0.3	1%	9.9 ± 0.3	2%	9.7 ± 0.3	4%	9.3 ± 0.3	8%
14GROR-25	10.5 ± 0.2	1%	10.6 ± 0.2	2%	10.3 ± 0.2	1%	10.0 ± 0.2	4%	9.7 ± 0.2	7%
14GROR-38	9.8 ± 0.3	0%	10.0 ± 0.3	2%	9.7 ± 0.3	1%	9.4 ± 0.3	4%	9.1 ± 0.3	7%
Between moraines, Lûtiviup Nunatarssua										
14GROR-10	9.2 ± 0.2	0%	9.4 ± 0.2	2%	9.1 ± 0.2	1%	8.9 ± 0.2	3%	8.6 ± 0.2	7%
14GROR-11	9.4 ± 0.2	0%	9.5 ± 0.2	1%	9.2 ± 0.2	2%	9.0 ± 0.2	4%	8.7 ± 0.2	7%
14GROR-12	9.2 ± 0.2	0%	9.3 ± 0.2	1%	9.1 ± 0.2	1%	8.8 ± 0.2	4%	8.5 ± 0.2	8%
Western stage, Qátqatsiaq										
14GROR-36	9.6 ± 0.2	0%	9.8 ± 0.2	2%	9.5 ± 0.2	1%	9.2 ± 0.2	4%	9.0 ± 0.2	6%
14GROR-37	10.0 ± 0.2	0%	10.2 ± 0.2	2%	9.9 ± 0.2	1%	9.6 ± 0.2	4%	9.3 ± 0.2	7%
Eastern stage, Qátqatsiaq										
14GROR-29	8.6 ± 0.2	0%	8.8 ± 0.2	2%	8.5 ± 170	1%	8.3 ± 0.2	3%	8.0 ± 0.2	7%
14GROR-30	9.4 ± 0.2	0%	9.5 ± 0.2	1%	9.2 ± 0.2	2%	9.0 ± 0.2	4%	8.7 ± 0.2	7%
14GROR-31	8.7 ± 0.2	0%	8.9 ± 0.2	2%	8.6 ± 0.2	1%	8.4 ± 0.2	3%	8.1 ± 0.2	7%
14GROR-32	9.0 ± 0.2	1%	9.1 ± 0.2	2%	8.8 ± 0.2	1%	8.6 ± 0.2	3%	8.3 ± 0.2	7%
14GROR-33	9.0 ± 0.2	0%	9.1 ± 0.2	1%	9.2 ± 0.2	2%	8.6 ± 0.2	4%	8.3 ± 0.2	8%
14GROR-34	9.3 ± 0.2	0%	9.5 ± 0.2	2%	9.2 ± 0.2	1%	8.9 ± 0.2	4%	8.7 ± 0.2	6%
14GROR-35	9.1 ± 0.2	0%	9.2 ± 0.2	1%	8.9 ± 0.2	2%	8.7 ± 0.2	4%	8.4 ± 0.2	8%
Inboard boulders, Qátqatsiaq										
14GROR-26	8.8 ± 0.2	0%	9.0 ± 0.2	2%	8.7 ± 0.2	1%	8.5 ± 0.2	3%	8.2 ± 0.2	7%
14GROR-27	9.1 ± 0.2	0%	9.2 ± 0.2	1%	9.0 ± 0.2	1%	9.0 ± 0.2	1%	8.4 ± 0.2	8%
14GROR-28	9.0 ± 0.2	0%	9.1 ± 0.2	1%	8.9 ± 0.2	1%	8.6 ± 0.2	4%	8.3 ± 0.2	8%

^a Young et al. (2013b).^b Balco (2017).^c Percent change from Arctic/Baffin Bay production rate and Lm scaling.

to the south (Fig. 2). There is a curvilinear end moraine just outside of the right lateral moraines which appears to have been formed by ice sourced from the northeast rather than Isuitsupkûa valley.

Between our two field sites, the moraines were mapped using air photographs and v2.0 (release 4) of the ArcticDEM. Large moraine crests were easily identifiable on air photographs, and we were able to trace the major moraines fairly continuously throughout the Søndre Isortoq region. Further mapping with the 2 m resolution ArcticDEM revealed many smaller moraine

segments that were not visible in the air photographs (Fig. 2). These moraine segments are limited in their lateral extent and cannot be correlated across the study area.

4.2. ¹⁰Be ages

We present ¹⁰Be ages from boulders at both sites in stratigraphic order, from the oldest to the youngest depositional events. ¹⁰Be ages from perched boulders beyond the moraines ($n = 9$) at both

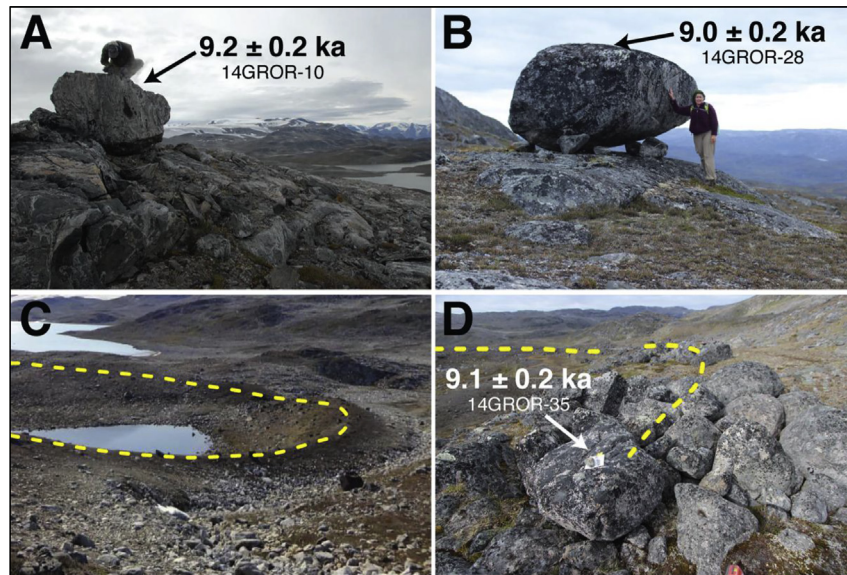


Fig. 3. (A) Boulder perched on bedrock between the moraines at Lûtiviup Nunatarssua. (B) Boulder perched on bedrock inside of the moraine at Qátqatsiaq. (C) Moraine (dashed yellow line) at Lûtiviup Nunatarssua. The moraine at this site is a well-defined, single-crested ridge. (D) Moraine boulder at Qátqatsiaq. The moraine at this site (dashed yellow line) is clast-supported and fragmented. (For interpretation of the references to colour in this figure legend, the reader is referred to the web version of this article.)

sites range from 9.9 ± 0.3 to 15.4 ± 0.5 ka (Table 1; Fig. 4). The average age of these boulders is 10.2 ± 0.2 ka ($n = 8$) after excluding one outlier (14GROR-05; 15.4 ± 0.5 ka) that is $> 3\sigma$ older than all other ^{10}Be ages. Two boulders from the outer end moraine fragment at the Qátqatsiaq site (Fig. 4B) have ^{10}Be ages of 9.6 ± 0.2 and 10.0 ± 0.2 ka, which average to 9.8 ± 0.3 ka. Boulders perched on bedrock between the western and eastern stage moraines at Lûtiviup Nunatarssua ($n = 3$; Fig. 4A) have ^{10}Be ages ranging from 9.2 ± 0.2 to 9.4 ± 0.2 ka, with an average of 9.3 ± 0.2 ka. Boulders on the lateral moraine crests ($n = 7$) at the Qátqatsiaq site yield ^{10}Be ages ranging from 8.6 ± 0.2 to 9.4 ± 0.2 ka (Fig. 4B), and average 9.0 ± 0.3 ka. At Qátqatsiaq, perched boulders inside of the moraines ($n = 3$) range from 8.8 ± 0.2 to 9.1 ± 0.2 ka, and average 9.0 ± 0.2 ka (Fig. 4B).

5. Discussion

5.1. Age of the Fjord Stade moraines in the Søndre Isortoq region

^{10}Be ages from perched boulders outside of the dated moraines at both sites reveal that ice retreated into the region at 10.2 ± 0.2 ka ($n = 8$). Deglaciation of the coast near Sisimuit, ~80 km west of the Søndre Isortoq region, occurred at 14.4 ± 0.9 ka (Winsor et al., 2015a). Using these values, we calculate an average retreat rate of 19.5 m a^{-1} from 14.4 to 10.3 ka, which is in accordance with early Holocene average retreat rates of $15\text{--}20 \text{ m a}^{-1}$ in this region (Rinterknecht et al., 2009; Winsor et al., 2015a).

The two boulders from the curvilinear end moraine at Qátqatsiaq have an average ^{10}Be age of 9.8 ± 0.3 ka (Fig. 4C). Because the end moraine is outboard of the more widely traceable lateral moraines and was likely formed by an older ice source, we would not necessarily expect the end moraine to have formed in the same depositional event as the lateral moraines despite their proximity. Indeed, the end moraine is ~0.8 kyr older than the lateral moraines at the Qátqatsiaq site (see below).

Due to the lack of suitable boulders directly on the moraines, the age of the western stage moraine at Lûtiviup Nunatarssua is constrained by perched boulders outside and inside of the moraine to between 10.4 ± 0.2 ($n = 2$) and 9.3 ± 0.2 ka ($n = 3$; Fig. 4A). Based on

the limited number of ^{10}Be ages at Lûtiviup Nunatarssua, the western stage moraine at this site appears to be older than the lateral moraines at Qátqatsiaq. The ages of inboard perched boulders at both sites overlap within dating uncertainty (Fig. 4C), and consequently we cannot discount the possibility that the moraines were deposited during the same event based on our ^{10}Be dating alone. However, taken together, our ^{10}Be ages and regional moraine map suggest that the western and eastern stage moraines were deposited in separate events. The western stage moraine at Lûtiviup Nunatarssua likely correlates with the curvilinear end moraine at Qátqatsiaq, which was deposited at 9.8 ± 0.3 ka. The eastern stage moraine, which formed after 9.3 ± 0.2 ka ($n = 2$), may correlate with the lateral moraine at Qátqatsiaq (see below).

At Qátqatsiaq, age control for the eastern stage moraines is provided by seven lateral moraine boulders that average 9.0 ± 0.3 ka. Further support for the ~9.0 ka age of these moraines is provided by ^{10}Be ages from perched boulders just inside of the moraines, which with an average exposure age of 9.0 ± 0.2 ka ($n = 3$), are identical to the moraine boulders themselves within dating uncertainty. Our finding that boulders just inboard of the moraines have the same ^{10}Be ages as the moraine boulders is consistent with what has been reported in the Disko Bugt Region (Young et al., 2013a). Given the tight clustering of the ^{10}Be ages from moraine boulders and inboard perched boulders (Fig. 4C), as well as the concordance with previously published age constraints (Ten Brink and Weidick, 1974), we have high confidence in our assignment of a ~9.0 ka age to the lateral moraines at Qátqatsiaq. Although we did not directly date the eastern stage moraine at Lûtiviup Nunatarssua, perched boulders outboard of the eastern stage indicate that it was deposited after 9.3 ± 0.2 ka ($n = 3$).

The absence of a prominent western stage moraine at Qátqatsiaq may result from similar lateral ice margin geometries during both early Holocene depositional events. Because the dated lateral moraines at this site are more than 20 km inland from our reconstructed early Holocene GrIS terminus (Fig. 2), retreat of the ice margin between the western and eastern moraine stages may not have caused substantial changes in ice thickness at the lateral moraine. As a result, the moraine deposited during the western stage could have been reoccupied during the eastern stage, as was

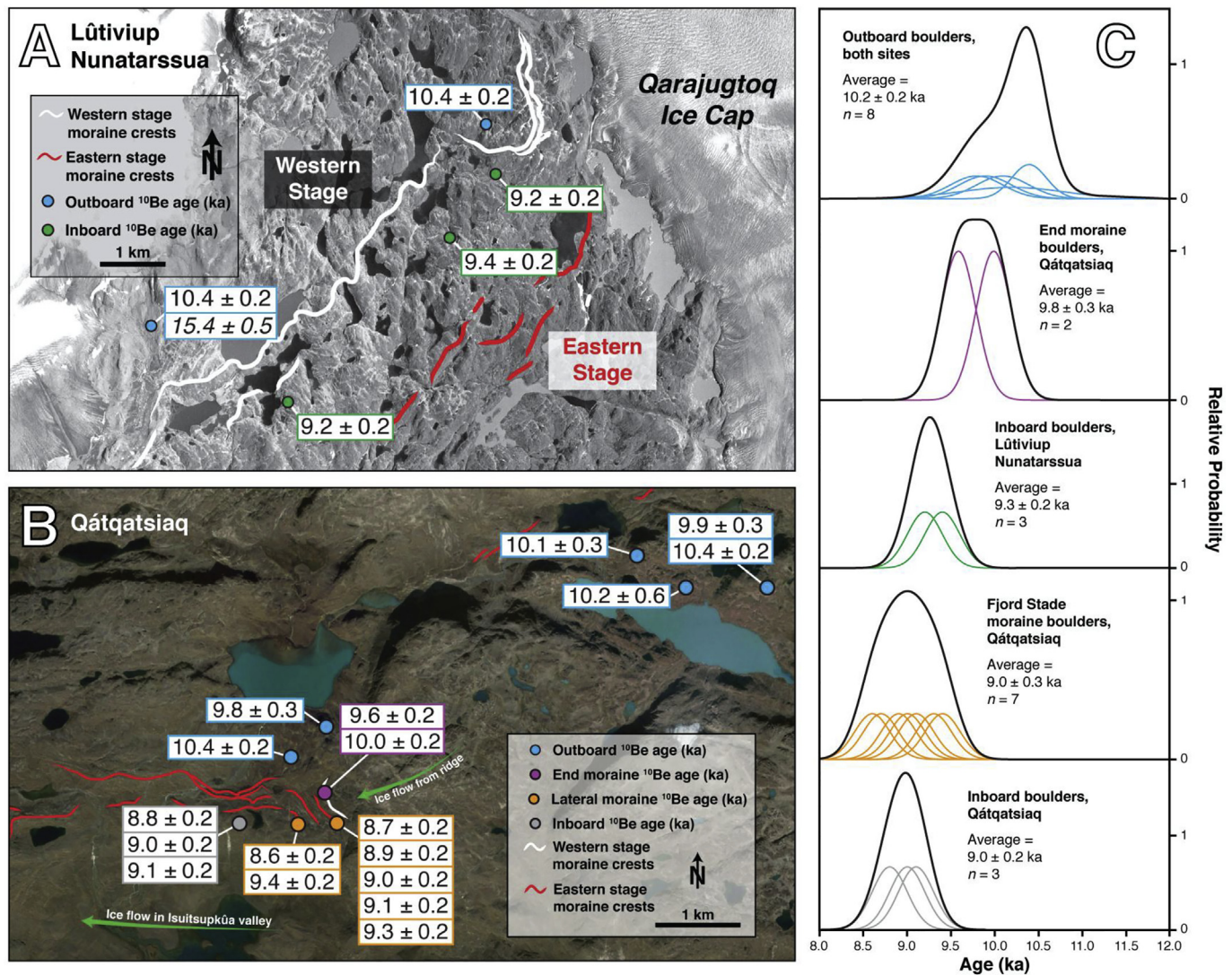


Fig. 4. (A) Lûtiviup Nunatarssua site showing western stage moraines (white lines), eastern stage moraines (red lines), and ^{10}Be ages (ka; 1SD uncertainty) from outside (blue dots) and between (green dots) the moraines. Base image: 1985 air photograph. (B) Qátqatsiaq site showing the western stage end moraine (white line) and the eastern stage lateral moraines (red lines). Also shown are sample locations and ^{10}Be ages (ka; 1SD uncertainty) from end moraine boulders (purple dots) and lateral moraine boulders (orange dots) as well as ^{10}Be ages from boulders outside (blue dots) and inside (gray dots) of the moraines. Base image: Google Earth. (C) Normal kernel density estimates of all ^{10}Be ages from the Søndre Isortoq region. Average of outboard boulders excludes one outlier (see Results section). (For interpretation of the references to colour in this figure legend, the reader is referred to the web version of this article.)

the case at the mouth of Jakobshavn Isfjord in the Disko Bugt region (Young et al., 2011b). This interpretation is supported by ^{10}Be ages of perched boulders just outside of the moraines, which indicate deglaciation at 10.2 ± 0.2 ka ($n = 8$). We argue that at both sites, the older moraine was deposited around 9.8 ± 0.7 ka, which is constrained by ^{10}Be ages of outboard perched boulders at both sites, ^{10}Be ages from the end moraine at Qátqatsiaq, and the inboard ^{10}Be ages from Lûtiviup Nunatarssua. A brief period of retreat from the older, western stage limit was followed by the younger, eastern stage readvance or stillstand, which culminated at 9.0 ± 0.3 ka.

The distribution of ^{10}Be ages beyond and inside the moraines in the Søndre Isortoq region suggests that moraine deposition may have occurred during a minor readvance of the GrIS margin rather than a stillstand. The 1.0–1.3 kyr gap between deglaciation of the landscape immediately outside of the moraines and the deposition of the moraines themselves suggests that the GrIS margin in the Søndre Isortoq region was not retreating continuously during this time (Young et al., 2013a), and instead reversed its overall pattern of

retreat to deposit the Fjord Stade moraine complex. This notion is supported by an air temperature reconstruction from a lake about 75 km north of our study area, which shows a prominent cooling event at ~ 8.2 ka and a shorter, less intense cooling events at ~ 9.4 and ~ 9.2 ka (Willemse and Törnqvist, 1999), suggesting that climate excursions recorded in Greenland ice cores were also expressed in the broader Sisimuit-Kangerlussuaq region. However, in the absence of additional geomorphic evidence of a readvance, such as a unit of minerogenic sediment in a threshold lake (Briner et al., 2010; Young et al., 2011a), we acknowledge that the ice margin may have experienced standstills during deposition of the Fjord Stade moraine complex.

5.2. Fjord Stade moraine deposition across western Greenland

Our minimum-limiting age of 9.3 ± 0.2 ka (inboard perched boulders; $n = 3$) for the western stage moraine at Lûtiviup Nunatarssua is compatible with the notion of a large-scale GrIS response

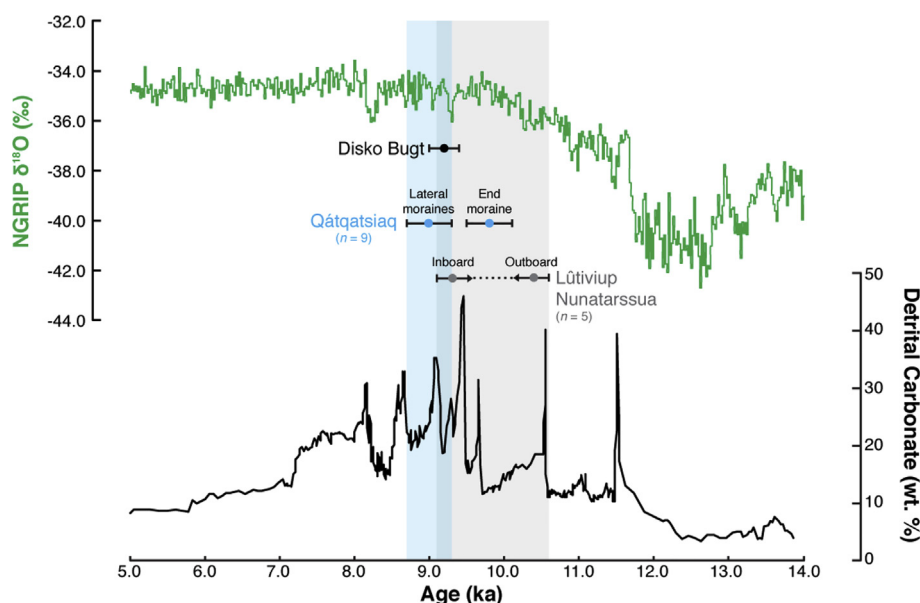


Fig. 5. NGRIP ice core $\delta^{18}\text{O}$ (green line; Vinther et al., 2006); age constraint on the Marrait moraine in the Disko Bugt region (black dot, 1SD; Young et al., 2013a); age constraints on the moraines at Qátqatsiaq (blue dots = average ages, showing 1SD of moraine boulder ages) and Lûtiviup Nunatarssua (gray dots = average ages, showing 1SD of bracketing boulder ages); and detrital carbonate content of marine sediment core MD99-2236 on the Labrador shelf (black line; Jennings et al., 2015). Vertical bars denote the two periods of moraine deposition in the Søndre Isortoq region, which took place at 9.0 ± 0.3 ka (blue bar) and 9.8 ± 0.7 ka (gray bar). (For interpretation of the references to colour in this figure legend, the reader is referred to the web version of this article.)

to early Holocene climate events. The western stage moraine at the Lûtiviup Nunatarssua site likely correlates to the ~ 9.8 ka end moraine at Qátqatsiaq (moraine boulders; $n = 2$), suggesting that the older moraine system was deposited at 9.8 ± 0.7 ka. Our mapping demonstrates that the 9.0 ± 0.3 ka moraine is also continuous throughout the Søndre Isortoq region (Fig. 2), and supports the hypothesis that a climatically-induced change in GrIS mass balance occurred in multiple locations across western Greenland around 9.0 ± 0.3 ka (Young et al., 2013a). Together with our updated moraine mapping, our ^{10}Be ages indicate that the GrIS near Søndre Isortoq experienced at least two regionally synchronous ice margin readvances or standstills during the early Holocene.

The western stage readvance or stillstand at 9.8 ± 0.7 ka may not have been restricted to the Søndre Isortoq region. The formation of the Taserqat moraines, located ~ 75 km north of the Søndre Isortoq region, has been constrained to between 10.5 and 9.3 cal kyr BP (Fig. 1; Weidick, 1972). The age of the western Fjord Stade moraine may also overlap with that of the Kapisigdlit Stade moraines in the Kangarsuneq Fjord region, which Larsen et al. (2014) constrained to ~ 10.2 ka.

Our age of 9.0 ± 0.3 ka for the eastern Fjord Stade moraine stage is indistinguishable within dating uncertainties from that of the Marrait moraine in the Disko Bugt region, which was dated to 9.2 ± 0.2 ka and lies more than 300 km away from our study area (Fig. 5; Young et al., 2011a, 2013a). The timing of Fjord Stade moraine deposition in both regions closely aligns with the 9.3 ka cooling event observed in Greenland ice cores (Rasmussen et al., 2007). This correspondence suggests that both land-terminating and marine-terminating GrIS margins responded in concert to the 9.3 ka event.

We did not identify a moraine in our field area that corresponds to the Tasiussaq moraine in the Disko Bugt region, which was dated to 8.2 ± 0.4 ka (Young et al., 2011a, 2013a). However, early Holocene retreat of this land-terminating sector of the western GrIS was punctuated by numerous minor readvances or stillstands of the ice

margin (Ten Brink, 1975). Consequently, moraine systems formed during successive stillstands may be separated by large distances. Indeed, the Umîvît-Keglen moraines, which lie ~ 50 km inland of the Fjord Stade moraines, have been suggested as Tasiussaq moraine equivalents (Winsor et al., 2015a), and therefore an 8.2 ka moraine may lie east of the Søndre Isortoq region.

The potential agreement between early Holocene moraine ages across western Greenland strongly implies that variations in regional climate (e.g., abrupt cooling during the 9.3 ka event) triggered the changes in mass balance that resulted in readvances or stillstands of broad regions of the western GrIS margin. Furthermore, these readvances or stillstands may have occurred in regions where the GrIS was marine-terminating (Disko Bugt, Kangarsuneq Fjord) and where it was land-terminating (Søndre Isortoq, Sisimuit-Kangerlussuaq), suggesting that large areas of GrIS margin responded to centennial-scale climatic perturbations regardless of terminal environment. Although the notion of a widespread response of the western GrIS to early Holocene abrupt cooling events is supported by the moraine chronologies in Søndre Isortoq and Disko Bugt, strong, direct evidence of a similar response to these events is lacking in other areas. This hypothesis could be further tested with additional moraine chronologies from western Greenland, particularly in the southern extent of the Fjord Stade moraines, where existing age controls conflict with one another (e.g., Weidick et al., 2012; Larsen et al., 2014).

5.3. Freshwater forcing of early Holocene GrIS margin change

Freshening of the North Atlantic is postulated to result in weakened overturning circulation and a slowdown or cessation of North Atlantic Deep Water formation, which would in turn weaken the subpolar gyre and reduce the strength of the relatively warm West Greenland Current, resulting in cooling in the Baffin Bay region (Alley and Agustsdottir, 2005; Kleiven et al., 2008). Freshwater input to the North Atlantic has been implicated in several prominent early Holocene abrupt cooling events, including the Preboreal

Oscillation (Fisher et al., 2002), the 9.3 ka event (Fleitmann et al., 2008), and the 8.2 ka event (Alley and Agustsdottir, 2005). Further evidence for freshwater forcing of early Holocene climate is provided by a marine core on the Labrador shelf. In this core, Jennings et al. (2015) identified prominent peaks in detrital carbonate content during the early to middle Holocene, which are interpreted as large freshwater pulses into the North Atlantic sourced from the Laurentide Ice Sheet via the Hudson Strait (Fig. 5). Several of these peaks correlate well with abrupt cooling events recorded in Greenland ice cores, supporting the notion that freshwater input into the North Atlantic can trigger cooling in the Baffin Bay region. The Labrador shelf detrital carbonate record also provides evidence for additional episodes of freshwater input to the North Atlantic during the early Holocene that are not strongly expressed in Greenland ice cores (Jennings et al., 2015). Four detrital carbonate peaks fall within the age range of both moraine systems in the Søndre Isortoq region (Fig. 5), suggesting a link between early Holocene freshwater forcing and GrIS margin behavior. Due to the lack of moraine boulders at the Lûtiviup Nunatarssua site and the relatively large uncertainty on our age estimate of the moraines, we cannot definitively determine which detrital carbonate peak, if any, is associated with the western Fjord Stade moraine.

The eastern Fjord Stade moraine, which dates to 9.0 ± 0.3 ka (moraine boulders, $n = 7$), may represent a response of the land-terminating GrIS margin to the 9.3 ka abrupt cooling event. The 9.3 ka event was the second largest cooling episode during the relatively warm Holocene epoch (Rasmussen et al., 2007). This short-lived event occurred between ~9350 and 9200 years ago and was first identified in the Greenland ice core record as an abrupt negative excursion in $\delta^{18}\text{O}$ (Vinther et al., 2006; Rasmussen et al., 2007; Fleitmann et al., 2008). High-resolution paleoclimate records across the Northern Hemisphere depict a distinct, widespread climatic anomaly during this time. A paleoproductivity-based air temperature reconstruction about 75 km north of our study area shows two short-lived cooling events at ~9.4 and ~9.2 ka (Willemse and Törnqvist, 1999). On Baffin Island, which lies across Baffin Bay from the Søndre Isortoq region, chironomid-based temperature reconstructions show cooling of about 3 °C at 9.2 cal kyr BP (Axford et al., 2009). In Europe, a drop in mean annual air temperature of 1.6 °C at ~9.2 cal kyr BP was reconstructed from deep-lake ostracods in the Bavarian Alps (von Grafenstein et al., 1999), and cooling at 9.3 cal kyr BP is shown in annually resolved German tree ring records (Spurk et al., 2002; Fleitmann et al., 2008). Farther afield, stalagmite $\delta^{18}\text{O}_{\text{calcite}}$ records from Oman and China exhibit a prominent positive anomaly at ~9.2 ka, indicating a reduction in Asian monsoon precipitation (Neff et al., 2001; Dykoski et al., 2005; Fleitmann et al., 2007).

This pattern of cooling in the North Atlantic and Europe with drying in Asia also occurred during the 8.2 ka event (Alley et al., 1997), suggesting a common forcing mechanism for the two cooling episodes. It has long been proposed that the trigger for the both the 9.3 and 8.2 ka events was a large freshwater outburst flood sourced from Laurentide Ice Sheet glacial lakes that drained into the North Atlantic Ocean (e.g., Teller and Leverington, 2004; Yu et al., 2010). Multiple proxies in the North Atlantic sedimentary record suggest that the region experienced considerable freshening and cooling during the 9.3 ka event, including an increase in ice-rafted debris (Bond et al., 2001) and changes in surface water Mg/Ca ratios and $\delta^{18}\text{O}$ (Came et al., 2007). Jennings et al. (2015) identified a detrital carbonate peak between 9.48 and 9.20 cal kyr BP (with maximum carbonate percentage at 9.46 cal kyr BP), indicating a Laurentide Ice Sheet-sourced freshwater pulse to the North Atlantic, which may be associated with the 9.3 ka event when considering age-model uncertainties. In addition, a ~45 m drop in

the relative lake level of Lake Superior at ~9.3 cal kyr BP, which delivered freshwater to the Labrador Sea via the Ottawa and St. Lawrence Rivers, has also been suggested as a trigger for the 9.3 ka event (Yu et al., 2010). Although the flux of water to the North Atlantic during the rapid drawdown of Lake Superior (~0.15 Sv; Yu et al., 2010) is substantially smaller than that of the outburst flood associated with the 8.2 ka event (~5.2 Sv; Teller and Leverington, 2004), we hypothesize that repeated release of meltwater into the Labrador Sea during the early Holocene (Jennings et al., 2015), particularly between 9.7 and 7.8 ka, increased the sensitivity of the North Atlantic by placing the system closer to the critical threshold needed to disrupt overturning circulation, weaken the West Greenland Current, and trigger cooling in the Baffin Bay region. Accordingly, even relatively small pulses of freshwater into the North Atlantic Ocean may have created the necessary conditions to generate readvances or standstills of the western GrIS during the early Holocene. Although directly testing this hypothesis is beyond the scope of this manuscript, it could be assessed with coupled ice sheet-ocean modeling.

A standstill spanning 350 km of the western GrIS as a result of the 9.3 ka event suggests that the broad regions of the GrIS are capable of responding to centennial-scale climate perturbations. Synchronous deposition of the Fjord Stade moraines across western Greenland, even along land-terminating margins, implies that substantial changes in western GrIS mass balance can be initiated by atmospheric cooling alone, and that the mass balance of the western GrIS was tightly coupled to early Holocene atmospheric temperatures (Young et al., 2013a). However, the muted response of land-terminating margins to early Holocene freshwater outburst events (i.e., a standstill or minor readvance in response to the 9.3 ka event) suggests that ocean forcing and glacier dynamics can amplify the response of marine-terminating margins to initial cooling.

6. Conclusions

Our new ^{10}Be chronology demonstrates that the GrIS in the Søndre Isortoq region experienced two minor readvances or still-stands at 9.8 ± 0.7 ka (bracketing boulders, $n = 5$, and two moraine boulders, $n = 2$) and 9.0 ± 0.3 ka (moraine boulders, $n = 7$). We propose that the land-terminating GrIS margin in the Søndre Isortoq region was sensitive to early Holocene freshwater outburst events in the North Atlantic, including the 9.3 ka abrupt cooling event. Synchronous deposition of the Fjord Stade moraine complex across at least 350 km of western Greenland, spanning from Disko Bugt in the north to Søndre Isortoq in the south, suggests a widespread response of the western GrIS to the 9.3 ka event. Furthermore, the response of the western GrIS to early Holocene freshwater forcing was not restricted to fast-flowing, marine-terminating outlet glaciers; the land-terminating margin in the Søndre Isortoq region halted its net retreat at least twice in response to North Atlantic freshwater outburst events (Jennings et al., 2015). Coupled with previously published ages from Disko Bugt (Young et al., 2013a), our results show that both land-terminating and marine-terminating sectors of the western GrIS responded to early Holocene abrupt cooling events, indicating that GrIS margins that are not dominated by dynamic processes are capable of responding to centennial-scale climate excursions. The response of a land-terminating margin to abrupt cooling episodes, including the 9.3 ka event, demonstrates that atmospheric forcing plays an important role in regulating the mass balance of the western GrIS on short, human-relevant timescales, although oceanic forcing and glacier dynamics can amplify the response of marine-terminating regions of the GrIS to climate fluctuations.

Atmospheric temperatures are expected to rise in the coming

centuries, particularly in the Arctic, and the tight coupling of the western GrIS margin with early Holocene temperature changes suggests that in the absence of other forcings, retreat of the ice sheet will continue. However, our results indicate that retreat of the broad areas of the western GrIS slowed at least twice in response to large inputs of freshwater into the North Atlantic Ocean during the early Holocene. As the Arctic warms, sustained melting of the GrIS and Arctic sea ice could introduce enough meltwater to the North Atlantic to alter ocean circulation patterns (e.g., Bamber et al., 2012), which could potentially offset further warming in the northern high latitudes (Hu et al., 2013). Nevertheless, additional age constraints on early Holocene ice margin change are needed to fully assess the sensitivity of the GrIS to North Atlantic freshwater forcing, which will ultimately improve predictions about the response of the GrIS to future climate change.

Acknowledgements

The authors thank Christina Ciaramerato and Nathaniel Lifton for assistance in the field, and Avriel Schweinsberg for assistance in both the field and the laboratory. We also thank Sandra O'Hara and Christopher Sbarra for assistance in the laboratory. Lee Corbett provided comments that improved the quality of this manuscript. Logistical support was provided by CH2M Hill Polar Field Services. This work was supported by the U.S. National Science Foundation (ARC-1204005).

Appendix A. Supplementary data

Supplementary data related to this article can be found at <https://doi.org/10.1016/j.quascirev.2017.11.028>.

References

- Alley, R.B., Agustsdottir, A.M., 2005. The 8k event: cause and consequences of a major Holocene abrupt climate change. *Quat. Sci. Rev.* 24 (10–11), 1123–1149.
- Alley, R.B., Mayewski, P.A., Sowers, T., Stuiver, M., Taylor, K.C., Clark, P.U., 1997. Holocene climatic instability: a prominent, widespread event 8200 yr ago. *Geology* 25 (6), 483–486.
- Aschwanden, A., Fahnestock, M.A., Truffer, M., 2016. Complex Greenland outlet glacier flow captured. *Nat. Commun.* 7.
- Axford, Y., Briner, J.P., Miller, G.H., Francis, D.R., 2009. Paleocological evidence for abrupt cold reversals during peak Holocene warmth on Baffin Island, Arctic Canada. *Quat. Res.* 71 (2), 142–149.
- Balco, G., April 2017. Production rate calculations for cosmic-ray-muon-produced ¹⁰Be and ²⁶Al benchmarked against geological calibration data. *Quat. Geochronol.* 39, 150–173.
- Balco, G., Briner, J., Finkel, R.C., Rayburn, J.A., Ridge, J.C., Schaefer, J.M., 2009. Regional beryllium-10 production rate calibration for late-glacial northeastern North America. *Quat. Geochronol.* 4 (2), 93–107.
- Balco, G., Stone, J.O., Lifton, N.A., Dunai, T.J., 2008. A complete and easily accessible means of calculating surface exposure ages or erosion rates from ¹⁰Be and ²⁶Al measurements. *Quat. Geochronol.* 3 (3), 174–195.
- Bamber, J., den Broeke, M., Ettema, J., Lenaerts, J., Rignot, E., 2012. Recent large increases in freshwater fluxes from Greenland into the North Atlantic. *Geophys. Res. Lett.* 39, 19.
- Beel, C.R., Lifton, N.A., Briner, J.P., Goehring, B.M., 2016. Quaternary evolution and ice sheet history of contrasting landscapes in Uummannaq and Sukkertoppen, western Greenland. *Quat. Sci. Rev.* 149, 248–258.
- Bennike, O., Björck, S., 2002. Chronology of the last recession of the Greenland ice sheet. *J. Quat. Sci.* 17 (3), 211–219.
- Bennike, O., Wagner, B., Richter, A., 2011. Relative sea level changes during the Holocene in the Sisimiut area, south-western Greenland. *J. Quat. Sci.* 26 (4), 353–361.
- Bindschadler, R.A., Nowicki, S., Abe-Ouchi, A., Aschwanden, A., Choi, H., Fastook, J., Granzow, G., Greve, R., Gutowski, G., Herzfeld, U., 2013. Ice-sheet model sensitivities to environmental forcing and their use in projecting future sea level (the SeaRISE project). *J. Glaciol.* 59 (214), 195–224.
- Bond, G., Kromer, B., Beer, J., Muscheler, R., Evans, M.N., Showers, W., Hoffmann, S., Lotti-Bond, R., Hajdas, I., Bonani, G., 2001. Persistent solar influence on North Atlantic climate during the Holocene. *Science* 294 (5549), 2130–2136.
- Briner, J.P., Stewart, H.A.M., Young, N.E., Philipps, W., Losee, S., 2010. Using proglacial-threshold lakes to constrain fluctuations of the Jakobshavn Isbræ ice margin, western Greenland, during the Holocene. *Quat. Sci. Rev.* 29 (27–28), 3861–3874.
- Came, R.E., Oppo, D.W., McManus, J.F., 2007. Amplitude and timing of temperature and salinity variability in the subpolar North Atlantic over the past 10 ky. *Geology* 35 (4), 315–318.
- Carlson, A.E., Winsor, K., Ullman, D.J., Brook, E.J., Rood, D.H., Axford, Y., LeGrande, A.N., Anslow, F.S., Sinclair, G., 2014. Earliest Holocene south Greenland ice sheet retreat within its late Holocene extent. *Geophys. Res. Lett.* 41 (15), 5514–5521.
- Carrivick, J.L., Yde, J., Russell, A.J., Quincey, D.J., Ingeman-Nielsen, T., Mallalieu, J., 2017. Ice-margin and meltwater dynamics during the mid-Holocene in the Kangerlussuaq area of west Greenland. *Boreas* 46, 369–387.
- Clark, P.U., Dyke, A.S., Shakun, J.D., Carlson, A.E., Clark, J., Wohlfarth, B., Mitrovica, J.X., Hostetler, S.W., McCabe, A.M., 2009. The last glacial maximum. *Science* 325 (5941), 710–714.
- Corbett, L.B., Bierman, P.R., Rood, D.H., 2016. An approach for optimizing in situ cosmogenic ¹⁰Be sample preparation. *Quat. Geochronol.* 33, 24–34.
- Corbett, L.B., Young, N.E., Bierman, P.R., Briner, J.P., Neumann, T.A., Rood, D.H., Graly, J.A., 2011. Paired bedrock and boulder ¹⁰Be concentrations resulting from early Holocene ice retreat near Jakobshavn Isfjord, western Greenland. *Quat. Sci. Rev.* 30 (13), 1739–1749.
- Csatho, B.M., Schenk, A.F., van der Veen, C.J., Babonis, G., Duncan, K., Rezvanbehbahani, S., van den Broeke, M.R., Simonsen, S.B., Nagarajan, S., van Angelen, J.H., 2014. Laser altimetry reveals complex pattern of Greenland Ice Sheet dynamics. *Proc. Natl. Acad. Sci.* 111 (52), 18478–18483.
- Dykoski, C.A., Edwards, R.L., Cheng, H., Yuan, D., Cai, Y., Zhang, M., Lin, Y., Qing, J., An, Z., Revenaugh, J., 2005. A high-resolution, absolute-dated Holocene and deglacial Asian monsoon record from Dongge Cave, China. *Earth Planet. Sci. Lett.* 233 (1), 71–86.
- Enderlin, E.M., Howat, I.M., Jeong, S., Noh, M.J., Angelen, J.H., Broeke, M.R., 2014. An improved mass budget for the Greenland ice sheet. *Geophys. Res. Lett.* 41 (3), 866–872.
- Fisher, T.G., Smith, D.G., Andrews, J.T., 2002. Preboreal oscillation caused by a glacial Lake Agassiz flood. *Quat. Sci. Rev.* 21 (8), 873–878.
- Fleitmann, D., Burns, S.J., Mangini, A., Mudelsee, M., Kramers, J., Villa, I., Neff, U., Al-Subbary, A.A., Buettner, A., Hippler, D., 2007. Holocene ITCZ and Indian monsoon dynamics recorded in stalagmites from Oman and Yemen (Socotra). *Quat. Sci. Rev.* 26 (1), 170–188.
- Fleitmann, D., Mudelsee, M., Burns, S.J., Bradley, R.S., Kramers, J., Matter, A., 2008. Evidence for a widespread climatic anomaly at around 9.2 ka before present. *Paleoceanography* 23 (1) (n/a–n/a).
- Funder, S., Kjeldsen, K.K., Kjaer, K.H., Cofaigh, C.O., 2011. The Greenland ice sheet during the past 300,000 Years: a review: quaternary glaciations - extent and chronology. *A Closer Look* 15, 699–713.
- Howat, I.M., Joughin, I., Scambos, T.A., 2007. Rapid changes in ice discharge from Greenland outlet glaciers. *Science* 315 (5818), 1559–1561.
- Hu, A., Meehl, G.A., Han, W., Yin, J., Wu, B., Kimoto, M., 2013. Influence of continental ice retreat on future global climate. *J. Clim.* 26 (10), 3087–3111.
- Jennings, A., Andrews, J., Pearce, C., Wilson, L., Ólafsdóttir, S., 2015. Detrital carbonate peaks on the Labrador shelf, a 13–7 ka template for freshwater forcing from the Hudson Strait outlet of the Laurentide Ice Sheet into the subpolar gyre. *Quat. Sci. Rev.* 107, 62–80.
- Kelley, S.E., Briner, J.P., Zimmerman, S.R., 2015. The influence of ice marginal setting on early Holocene retreat rates in central West Greenland. *J. Quat. Sci.* 30 (3), 271–280.
- Kelly, M., 1985. A Review of the Quaternary Geology of Western Greenland: Quaternary Environments Eastern Canadian Arctic, Baffin Bay and Western Greenland. Allen and Unwin, Boston, pp. 461–501.
- Kelly, M.A., Lowell, T.V., 2009. Fluctuations of local glaciers in Greenland during latest Pleistocene and Holocene time. *Quat. Sci. Rev.* 28 (21–22), 2088–2106.
- Kleiven, H.K.F., Kissel, C., Laj, C., Ninnemann, U.S., Richter, T.O., Cortijo, E., 2008. Reduced North Atlantic deep water coeval with the glacial Lake Agassiz freshwater outburst. *Science* 319 (5859), 60–64.
- Kohl, C.P., Nishiizumi, K., 1992. Chemical isolation of quartz for measurement of in situ -produced cosmogenic nuclides. *Geochimica Cosmochimica Acta* 56 (9), 3583–3587.
- Lal, D., 1991. Cosmic ray labeling of erosion surfaces: in situ nuclide production rates and erosion models. *Earth Planet. Sci. Lett.* 104 (2–4), 424–439.
- Larsen, N.K., Funder, S., Kjaer, K.H., Kjeldsen, K.K., Knudsen, M.F., Linde, H., 2014. Rapid early Holocene ice retreat in West Greenland. *Quat. Sci. Rev.* 92, 310–323.
- Larsen, N.K., Funder, S., Linde, H., Möller, P., Schomacker, A., Fabel, D., Xu, S., Kjaer, K.H., 2016. A Younger Dryas re-advance of local glaciers in north Greenland. *Quat. Sci. Rev.* 147, 47–58.
- Levy, L.B., 2014. Late Glacial and Holocene Fluctuations of Local Glaciers and the Greenland Ice Sheet, Eastern and Western Greenland. Dartmouth College.
- Levy, L.B., Kelly, M.A., Howley, J.A., Virginia, R.A., 2012. Age of the Orkenden moraines, Kangerlussuaq, Greenland: constraints on the extent of the south-western margin of the Greenland ice sheet during the Holocene. *Quat. Sci. Rev.* 52, 1–5.
- Long, A.J., Roberts, D.H., Dawson, S., 2006. Early Holocene history of the West Greenland ice sheet and the GH-8.2 event. *Quat. Sci. Rev.* 25 (9–10), 904–922.
- Morlighem, M., Rignot, E., Mouginot, J., Seroussi, H., Larour, E., 2014. Deeply incised submarine glacial valleys beneath the Greenland ice sheet. *Nat. Geosci.* 7 (6).
- Neff, U., Burns, S., Mangini, A., Mudelsee, M., Fleitmann, D., Matter, A., 2001. Strong coherence between solar variability and the monsoon in Oman between 9 and 6 kyr ago. *Nature* 411 (6835), 290–293.

- Nick, F.M., Vieli, A., Andersen, M.L., Joughin, I., Payne, A., Edwards, T.L., Pattyn, F., van de Wal, R.S.W., 2013. Future sea-level rise from Greenland's main outlet glaciers in a warming climate. *Nature* 497 (7448), 235–238.
- Nishiizumi, K., Imamura, M., Caffee, M.W., Southon, J.R., Finkel, R.C., McAninch, J., 2007. Absolute calibration of 10Be AMS standards. *Nucl. Instrum. Methods Phys. Res. Sect. B Beam Interact. Mater. Atoms* 258 (2), 403–413.
- Pfeffer, W.T., Harper, J.T., O'Neel, S., 2008. Kinematic constraints on glacier contributions to 21st-century sea-level rise. *Science* 321 (5894), 1340–1343.
- Price, S.F., Payne, A.J., Howat, I.M., Smith, B.E., 2011. Committed sea-level rise for the next century from Greenland ice sheet dynamics during the past decade. *Proc. Natl. Acad. Sci.* 108 (22), 8978–8983.
- Putnam, A., Schaefer, J., Barrell, D., Vandergoes, M., Denton, G., Kaplan, M., Finkel, R., Schwartz, R., Goehring, B., Kelley, S., 2010. In situ cosmogenic 10 Be production-rate calibration from the Southern Alps, New Zealand. *Quat. Geochronol.* 5 (4), 392–409.
- Rasmussen, S.O., Vinther, B.M., Clausen, H.B., Andersen, K.K., 2007. Early Holocene climate oscillations recorded in three Greenland ice cores. *Quat. Sci. Rev.* 26 (15–16), 1907–1914.
- Rignot, E., Box, J.E., Burgess, E., Hanna, E., 2008. Mass balance of the Greenland ice sheet from 1958 to 2007. *Geophys. Res. Lett.* 35 (20), L20502.
- Rinterknecht, V., Gorokhov, Y., Schaefer, J., Caffee, M., 2009. Preliminary 10Be chronology for the last deglaciation of the western margin of the Greenland Ice Sheet. *J. Quat. Sci.* 24 (3), 270–278.
- Roberts, D.H., Long, A.J., Schnabel, C., Davies, B.J., Xu, S., Simpson, M.J.R., Schwartz, R., 2009. Ice sheet extent and early deglacial history of the southwestern sector of the Greenland Ice Sheet. *Quat. Sci. Rev.* 28 (25–26), 2760–2773.
- Shepherd, A., Ivins, E.R., Geruo, A., Barletta, V.R., Bentley, M.J., Bettadpur, S., Briggs, K.H., Bromwich, D.H., Forsberg, R., Galin, N., 2012. A reconciled estimate of ice-sheet mass balance. *Science* 338 (6111), 1183–1189.
- Sinclair, G., Carlson, A.E., Mix, A.C., Lecavalier, B.S., Milne, G., Mathias, A., Buizert, C., DeConto, R., 2016. Diachronous retreat of the Greenland ice sheet during the last deglaciation. *Quat. Sci. Rev.* 145, 243–258.
- Sole, A., Payne, T., Bamber, J., Nienow, P., Krabill, W., 2008. Testing hypotheses of the cause of peripheral thinning of the Greenland Ice Sheet: is land-terminating ice thinning at anomalously high rates? *Cryosphere* 2 (2), 205–218.
- Spurk, M., Leuschner, H.H., Baillie, M.G., Briffa, K.R., Friedrich, M., 2002. Depositional frequency of German subfossil oaks: climatically and non-climatically induced fluctuations in the Holocene. *Holocene* 12 (6), 707–715.
- Stone, J.O., 2000. Air pressure and cosmogenic isotope production. *J. Geophys. Res. Solid Earth* 105 (B10), 23753–23759.
- Sugden, D., 1972. Deglaciation and isostasy in the Sukkertoppen ice cap area, West Greenland. *Arct. Alp. Res.* 97–117.
- Teller, J.T., Leverington, D.W., 2004. Glacial Lake Agassiz: a 5000 yr history of change and its relationship to the $\delta^{18}\text{O}$ record of Greenland. *Geol. Soc. Am. Bull.* 116 (5–6), 729–742.
- Ten Brink, N.W., 1975. Holocene history of the Greenland ice sheet based on radiocarbon-dated moraines in West Greenland. *Meddelelser Om. Grønland* 44, 113.
- Ten Brink, N.W., Weidick, A., 1974. Greenland ice sheet history since the last glaciation. *Quat. Res.* 4 (4), 429–440.
- Van Tatenhove, F.G.M., 1995. The Dynamics of Holocene Deglaciation in West Greenland with Emphasis on Recent Ice Marginal Proglaciations.
- Vieli, A., Nick, F.M., 2011. Understanding and modelling rapid dynamic changes of tidewater outlet glaciers: issues and implications. *Surv. Geophys.* 32 (4–5), 437–458.
- Vinther, B.M., Clausen, H.B., Johnsen, S.J., Rasmussen, S.O., Andersen, K.K., Buchardt, S.L., Dahl-Jensen, D., Seierstad, I.K., Siggaard-Andersen, M.L., Steffensen, J.P., 2006. A synchronized dating of three Greenland ice cores throughout the Holocene. *J. Geophys. Res. Atmos.* 111, D13.
- von Grafenstein, U., Erlenkeuser, H., Brauer, A., Jouzel, J., Johnsen, S.J., 1999. A mid-European decadal isotope-climate record from 15,500 to 5000 years BP. *Science* 284 (5420), 1654–1657.
- Warren, C.R., Hulton, N.R.J., 1990. Topographic and glaciological controls on Holocene ice-sheet margin dynamics, central West Greenland. *Ann. Glaciol.* 14, 307–310.
- Weidick, A., 1968. Observations on Some Holocene Glacier Fluctuations in West Greenland. *Nyt Nordisk Forlag, Copenhagen, Denmark, Meddelelser om Grønland*, p. 202.
- Weidick, A., 1972. Holocene Shorelines and Glacial Stages in Greenland: an Attempt at Correlation. *Copenhagen, Grønlands Geologiske Undersøgelse, Grønlands Geologiske Undersøgelse*, p. 39.
- Weidick, A., 1985. Review of glacier changes in west Greenland. *Z. für Gletscherkd. Glaziogeologie* 21, 301–309.
- Weidick, A., Bennike, O., Citterio, M., Norgaard-Pedersen, N., 2012. Neoglacial and historical glacier changes around Kangarsuneq fjord in southern West Greenland. *Geol. Surv. Den. Grønland Bull.* 27, 61.
- Willemse, N.W., Törnqvist, T.E., 1999. Holocene century-scale temperature variability from West Greenland lake records. *Geology* 27 (7), 580–584.
- Winsor, K., Carlson, A.E., Caffee, M.W., Rood, D.H., 2015a. Rapid last-deglacial thinning and retreat of the marine-terminating southwestern Greenland ice sheet. *Earth Planet. Sci. Lett.* 426, 1–12.
- Winsor, K., Carlson, A.E., Welke, B.M., Reilly, B., 2015b. Early deglacial onset of southwestern Greenland ice-sheet retreat on the continental shelf. *Quat. Sci. Rev.* 128, 117–126.
- Young, N.E., Briner, J.P., Axford, Y., Csatho, B., Babonis, G.S., Rood, D.H., Finkel, R.C., 2011a. Response of a marine-terminating Greenland outlet glacier to abrupt cooling 8200 and 9300 years ago. *Geophys. Res. Lett.* 38 (24), L24701.
- Young, N.E., Briner, J.P., Rood, D.H., Finkel, R.C., Corbett, L.B., Bierman, P.R., 2013a. Age of the Fjord Stade moraines in the Disko Bugt region, western Greenland, and the 9.3 and 8.2 ka cooling events. *Quat. Sci. Rev.* 60, 76–90.
- Young, N.E., Briner, J.P., Stewart, H.A.M., Axford, Y., Csatho, B., Rood, D.H., Finkel, R.C., 2011b. Response of Jakobshavn Isbrae, Greenland, to Holocene climate change. *Geol. (Boulder)* 39 (2), 131–134.
- Young, N.E., Schaefer, J.M., Briner, J.P., Goehring, B.M., 2013b. A 10Be production-rate calibration for the Arctic. *J. Quat. Sci.* 28 (5), 515–526.
- Yu, S.-Y., Colman, S.M., Lowell, T.V., Milne, G.A., Fisher, T.G., Breckenridge, A., Boyd, M., Teller, J.T., 2010. Freshwater outburst from Lake Superior as a trigger for the cold event 9300 years ago. *Science* 328 (5983), 1262–1266.